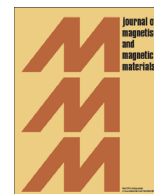




ELSEVIER

Contents lists available at ScienceDirect

## Journal of Magnetism and Magnetic Materials

journal homepage: [www.elsevier.com/locate/jmmm](http://www.elsevier.com/locate/jmmm)

# Ferromagnetic ordering in $\text{NpAl}_2$ : Magnetic susceptibility and $^{27}\text{Al}$ nuclear magnetic resonance

L. Martel\*, J.-C. Griveau, R. Eloirdi, C. Selfslag, E. Colineau, R. Caciuffo

European Commission, Joint Research Centre (JRC), Institute for Transuranium Elements (ITU), P.O. Box 2340, D-76125 Karlsruhe, Germany



## ARTICLE INFO

## Article history:

Received 20 February 2015

Received in revised form

12 March 2015

Accepted 25 March 2015

Available online 28 March 2015

## Keywords:

Magnetic susceptibility

 $^{27}\text{Al}$  NMR

Low temperature

Neptunium

Intermetallic

Ferromagnetism

## ABSTRACT

We report on the magnetic properties of the neptunium based ferromagnetic compound  $\text{NpAl}_2$ . We used magnetization measurements and  $^{27}\text{Al}$  NMR spectroscopy to access magnetic features related to the paramagnetic and ordered states ( $T_C=56$  K). While very precise DC SQUID magnetization measurements confirm ferromagnetic ordering, they show a relatively small hysteresis loop at 5 K reduced with a coercive field  $H_{Co}\sim 3000$  Oe. The variable offset cumulative spectra (VOCS) acquired in the paramagnetic state show a high sensitivity of the  $^{27}\text{Al}$  nuclei spectral parameters (Knight shifts and line broadening) to the ferromagnetic ordering, even at room temperature.

© 2015 The Authors. Published by Elsevier B.V. This is an open access article under the CC BY-NC-ND license (<http://creativecommons.org/licenses/by-nc-nd/4.0/>).

## 1. Introduction

Accessing ground state properties of transuranium compounds is an important challenge from both theoretical and application-related perspectives. Indeed, expanding the knowledge data base on basic properties of nuclear fuels and related compounds is needed to elaborate reliable safety assessment models with predictive capabilities. A wide range of macroscopic and microscopic techniques are available for investigating structural, thermodynamic and electronic properties of nuclear materials, but in many cases the unavoidable presence of lattice defects created by self-irradiation damage hinders establishing unambiguous correlations between microscopic and macroscopic behavior. This is a common feature of actinide-based compounds, for which further difficulties are introduced by the intrinsic dual nature of the electrons with 5f parentage. Being at the verge of an instability between a localized and a delocalized regime, 5f electrons are indeed extremely sensitive to varying parameters such as pressure, temperature, magnetic field, or doping [1,2].

Nuclear Magnetic Resonance (NMR) spectroscopy is a powerful technique for the investigating of magnetic and electronic properties in solid-state matter. For the actinide series two nuclei are of practical use, namely  $^{235}\text{U}$  [3,4] ( $I=7/2$ ) and  $^{239}\text{Pu}$  [5] ( $I=1/2$ ), but unfortunately only at very low temperatures because the very fast spin-lattice relaxation rate makes the signal vanish quickly with

increasing temperature (e.g. no signal was detected above 14 K for  $^{235}\text{U}$ ). Few installations exist around the world where NMR studies can be carried out on nuclear materials [5–10]. Here, we focus on a model compound and examine its magnetic properties by magnetization, susceptibility, and low-temperature NMR measurements. Neptunium dialuminide,  $\text{NpAl}_2$ , is a transuranium intermetallic compound exhibiting the cubic Laves phase crystal structure (space group  $\text{Fd}\bar{3}m$ ), and showing long-range ferromagnetic order below its Curie temperature  $T_C=56$  K [11,12]. It contrasts to its isostructural actinide dialuminides,  $\text{UAl}_2$  and  $\text{PuAl}_2$ , which have been extensively studied as prototypes of spin fluctuator systems [13] with a not yet confirmed magnetic order at  $\sim 3.5$  K in the case of  $\text{PuAl}_2$  [14]. Due to its large localized magnetic moment [11,15] corresponding to an hyperfine magnetic field of 330 T at 4.2 K,  $\text{NpAl}_2$  is a well-known reference material for velocity calibration in Mössbauer spectroscopy [16,17]. An NMR report on 5f-electron localization in the actinides published by Fradin in 1976 barely mentioned NMR of  $\text{NpAl}_2$  suggesting a strongly localized system due to large variations of the NMR parameters (Knight Shift) with temperature [18]. It is interesting to notice that insertion of palladium into its crystallographic structure leads to the formation of the only known Np-based superconductor, namely  $\text{NpPd}_5\text{Al}_2$  (body-centered  $\text{ZrNi}_2\text{Al}_5$ -type tetragonal structure, with space group:  $I4/mmm$ ) [19–21].

\* Corresponding author.

E-mail address: [laura.martel@ec.europa.eu](mailto:laura.martel@ec.europa.eu) (L. Martel).

## 2. Experimental

### 2.1. Synthesis and characterization

The samples were synthesized by arc melting stoichiometric amounts of constituent metals (Np 3N, Al 5N) in a high purity argon atmosphere on a water cooled copper plate, using a Zr metal button as an oxygen getter. The sample was annealed at 800 °C for 24 h to remove any effect of radiation damages. The homogeneity of  $\text{NpAl}_2$  was checked by powder X-ray diffraction (XRD) using a dedicated Bruker D8 Advance diffractometer (Cu  $\text{K}\alpha_1$  radiation, 40 kV, and 40 mA), installed in a radioactive glovebox and equipped with a curved Ge monochromator (1, 1, 1) and a Lynxeye linear position-sensitive detector. Powder diffraction patterns were recorded using a step size of  $0.0197^\circ$  spanning the angular range of  $10^\circ \leq 2\theta \leq 120^\circ$ . About 20 mg of powder was loaded in an epoxy resin to prevent dispersion. The results showed a single well-crystallized with temperature with room temperature lattice parameter  $a = 0.77909$  (7) nm, very close to the value reported in the literature (0.7785 nm, Aldred et al. [11]).

### 2.2. Magnetic properties

Magnetic susceptibility measurements were carried out in the temperature range 2–300 K, with an external magnetic field up to 7 T on a 66.1 mg sample using the MPMS-7 SQUID from Quantum Design (QD). For these DC magnetization measurements, the sample was encapsulated in a Plexiglas container contributing a low magnetic signal. Subtraction of the background and calibration were performed following a standard procedure.

### 2.3. NMR

The  $^{27}\text{Al}$  spectra were recorded on a Bruker NMR spectrometer at the frequency of 104.3 MHz (static field of 9.4 T). Due to its high radiotoxicity, the  $\text{NpAl}_2$  sample used for the NMR experiments was encapsulated in a double container (Fig. 1A). In addition, the in-, out-helium gas flow valves, and the security exit valve of the static 7 mm Bruker NMR cryoprobe were all connected to the environment gas lines by absolute filters (Fig. 1B and C).

Due to their broadness, spectra were acquired using a variable offset cumulative spectrum (VOCS) technique [22]. A total of 96 individual Hahn echo spectra with frequency offsets in step of 16.5 kHz were required to obtain the full spectrum (i.e. central and satellite transitions) at room temperature. At lower temperatures, only the central line and the first satellite transitions were acquired. The NMR spectra were reconstructed and analyzed using the DMfit software [23].

## 3. Results and discussions

### 3.1. Magnetization

The normalized magnetic susceptibility,  $\chi = M/H$ , of  $\text{NpAl}_2$ , is presented in Fig. 2, together with the inverse susceptibility  $\chi^{-1}$ , obtained in the paramagnetic state as the ratio  $H/M$  between applied field and magnetization. The magnetic order is determined by the peak observed on the ZFC curves of magnetic field at very low field. Inset of Fig. 2 shows the measurements at 100 Oe, confirming the ordering temperature  $T_C = 56$  K. Above 80 K,  $\chi^{-1}$  (T) (determined with an applied field  $\mu_0 H = 7$  T) can be well fitted (see inset in Fig. 2) by a Curie–Weiss law [24],  $\chi^{-1} = (T - \theta_p)/C$ , yields a paramagnetic Curie temperature  $\theta_p \sim 72$  K, which is comparable to  $T_C$  and in good agreement with the results of Aldred et al. [12]. The effective magnetic moment deduced from the Curie constant  $C$ ,

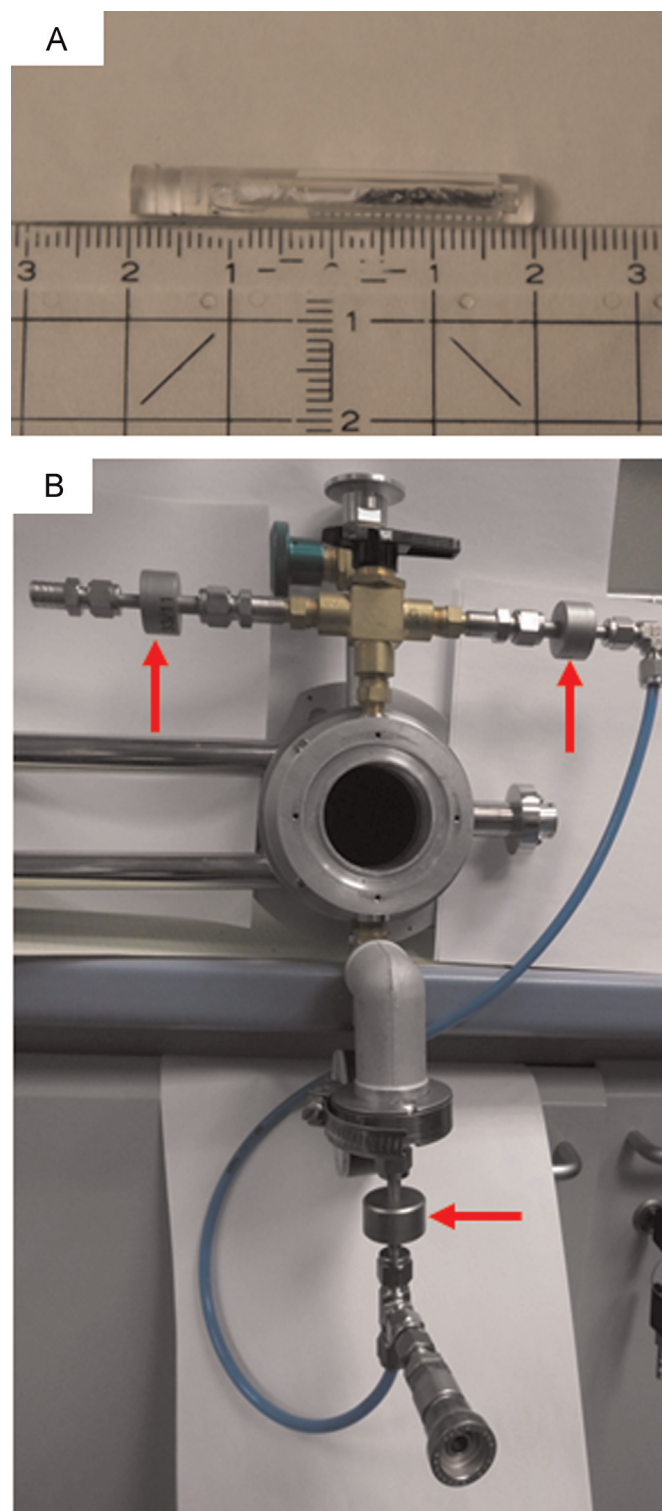


**Fig. 1.** Bulk  $\text{NpAl}_2$  encapsulated in a double container used for the NMR experiments, (A). Modified low temperature NMR probe with in- and out-helium gas flow valves, and the security exit valve with their absolute filters (B). The filters are indicated by red arrows. (For interpretation of the references to color in this figure legend, the reader is referred to the web version of this article.)

$\mu_{\text{eff}} \sim 2.1 \mu_B/\text{Np}$ , is also consistent with previous studies [25]. This value is smaller than that calculated for the free ion  $\text{Np}^{3+}$  in Russell-Saunders coupling ( $2.68 \mu_B/\text{Np}$ ). This reduction of  $\mu_{\text{eff}}$  with respect to the free ion value has been attributed to the crystal field interaction [12]. Fig. 3 presents magnetic hysteresis loops, obtained at 5 K in the ordered state. The coercive field is relatively

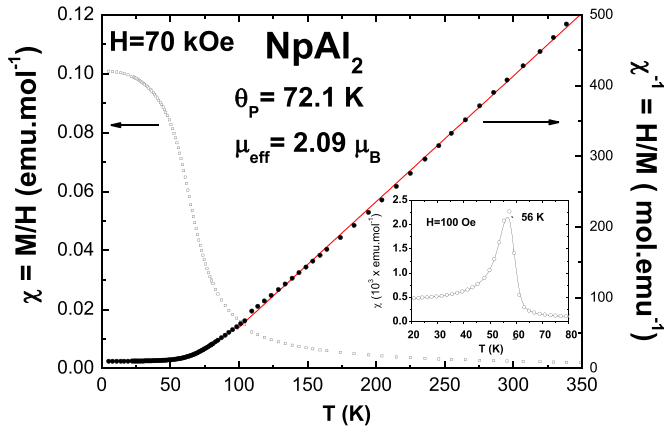


Fig. 2.  $\text{NpAl}_2$  magnetic susceptibility,  $\chi=M/H$  (left), and inverse magnetic susceptibility,  $1/\chi$ , (right) with its corresponding Curie–Weiss law fit from 100 to 300 K (red line) determined at 70 kOe. Inset shows the ZFC magnetic susceptibility determined at 100 Oe, showing the magnetic order at 56 K. (For interpretation of the references to color in this figure legend, the reader is referred to the web version of this article.)

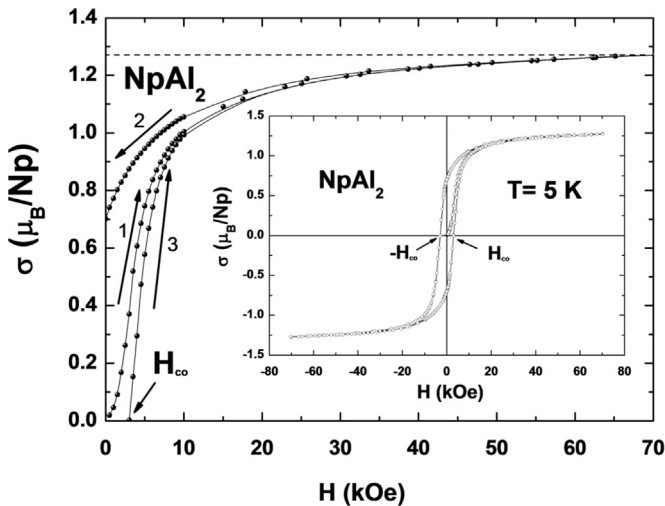


Fig. 3. Magnetization curves of  $\text{NpAl}_2$  measured at 5 K. The magnetization is not completely saturated at 70 kOe at this temperature. The figure shows the first magnetization curve (1) and those recorded with decreasing (2) and increase after (3) magnetic field. Inset: complete hysteresis loop curve at 5 K showing a small coercive field ( $H_{co} \sim 3000$  Oe).

small for a ferromagnet ( $H_{co} \sim 3000$  Oe) stressing the absence of strongly pinned magnetic domains in the material in the ordered state. An estimation of the saturated magnetic moment, by taking magnetization values at 5 K and 7 T, gives  $\mu_{sat} \sim 1.2 \mu_B$ , which is close to the saturation of the Np moment previously determined by Aldred et al. [12] by magnetization and slightly smaller than the ordered moment derived from neutrons diffraction and Mössbauer spectroscopy. This reduction of the saturated/ordered moment compared to the  $\text{Np}^{3+}$  free ion value of  $2.4 \mu_B$  expected for Russell-Saunders coupling could then arise from a partial delocalization of 5f-electrons, as suggested by recent electronic structure calculations [21] and in agreement with the observed value of the effective moment.

### 3.2. NMR

Fig. 4 presents the full  $^{27}\text{Al}$  NMR spectrum acquired at room temperature by summing 96 spectra. It is characteristic of a quadrupolar perturbed powder pattern with its central and satellite transitions. While the satellite transitions present

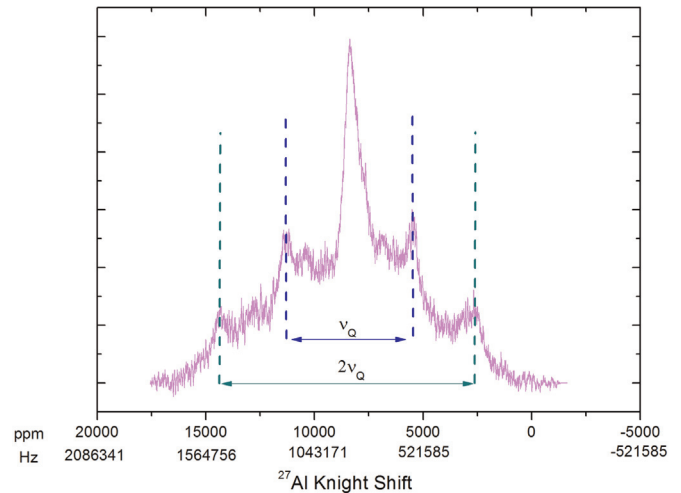


Fig. 4.  $^{27}\text{Al}$  VOCS-NMR spectrum of  $\text{NpAl}_2$  obtained by summing 96 spectra at room temperature.

singularities characteristic of a  $\eta=0$  symmetry [26], the central transition does not present the expected characteristic singularities observed for example in  $\text{UAl}_2$  and  $\text{PuAl}_2$  [13]. The nuclear quadrupolar frequency,  $\nu_Q$ , has been determined considering the satellite transitions and using the second-order perturbation theory for a spin 5/2 stating that the distance between the  $-3/2 \leftrightarrow -1/2$  and the  $1/2 \leftrightarrow 3/2$  transitions corresponds to  $\nu_Q$  and the distance between the  $-5/2 \leftrightarrow -3/2$  and the  $3/2 \leftrightarrow 5/2$  transitions corresponds to  $2\nu_Q$  (see Fig. 4). A value of 0.621 MHz (i.e. for  $I=5/2$ ,  $C_Q=20\nu_Q/3=4.1$  MHz) has been found. This value is similar to that determined by Arko et al. [13] for  $\text{UAl}_2$  ( $C_Q=4.71$  MHz,  $\nu_Q=0.706$  MHz) and  $\text{PuAl}_2$  ( $C_Q=3.78$  MHz,  $\nu_Q=0.567$  MHz) [13,27,28], or to the isostructural rare earth antiferromagnetic  $\text{CeAl}_2$  ( $C_Q=4.8$  MHz,  $\nu_Q=0.72$  MHz) [29,30] and ferromagnetic  $\text{GdAl}_2$  ( $C_Q=4.67$  MHz,  $\nu_Q=0.7$  MHz) [31]. Nevertheless, the central-band possesses a full width at half maximum (FWHM) of 113 kHz contrary to that of 3 kHz previously published for  $\text{UAl}_2$  and  $\text{PuAl}_2$ . The first explanation for this larger FWHM is an electronic effect due to the oxidation state  $\sim\text{III}$  for Np in contrast to IV for U and Pu. To our knowledge, only one NMR experiment, made on skutterudite  $\text{NpFe}_4\text{P}_{12}$  ( $\text{Np}^{4+}$ ,  $5f^3$ ), referred to the study of a ferromagnetic neptunium-based compound [9,10] and our data cannot unfortunately be compared to  $\text{NpFe}_4\text{P}_{12}$  due to the different oxidation state. The second explanation, is the possible sensing by the  $^{27}\text{Al}$  nuclei of the ferromagnetic ordering already at room temperature as this effect can be visible in the NMR spectrum well above the ordering temperature [32,33]. Both propositions are discussed later in the text.

Variations of the  $^{27}\text{Al}$  ( $-1/2 \leftrightarrow 1/2$ ) and ( $-3/2 \leftrightarrow 3/2$ ) transitions spectra in the range 300–140 K are presented in Fig. 5. Our experiments were performed in the paramagnetic state, as below 140 K the signal moves outside the frequency range fixed by our commercial NMR probe. The  $\nu_Q$  obtained considering the distance between the  $-3/2 \leftrightarrow -1/2$  and the  $1/2 \leftrightarrow 3/2$  transitions is constant for the temperature range considered excluding the possibility of lattice distortion with decreasing temperature. Fig. 6 and its inset show the temperature dependence of the  $^{27}\text{Al}$  Knight shift ( $^{27}\text{K}$ ) and its correlation with the magnetic susceptibility. Due to the very important broadening previously discussed, the  $^{27}\text{K}$  was determined using the gravity center position given by the DMfit software.  $^{27}\text{K}$  increases very fast as the temperature decreases and can be attributed mainly to transferred hyperfine fields from the Np 5f-electrons on the  $^{27}\text{Al}$  nuclei. Therefore, the following equation can be considered [10,34]:

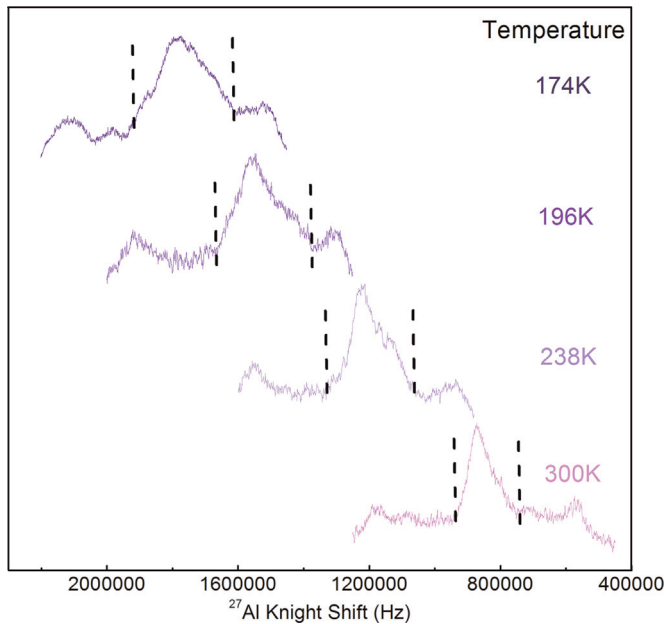


Fig. 5. Variations of the  $^{27}\text{Al}$  ( $-1/2 \leftrightarrow 1/2$ ) and ( $-3/2 \leftrightarrow 3/2$ ) transitions spectra with temperature.

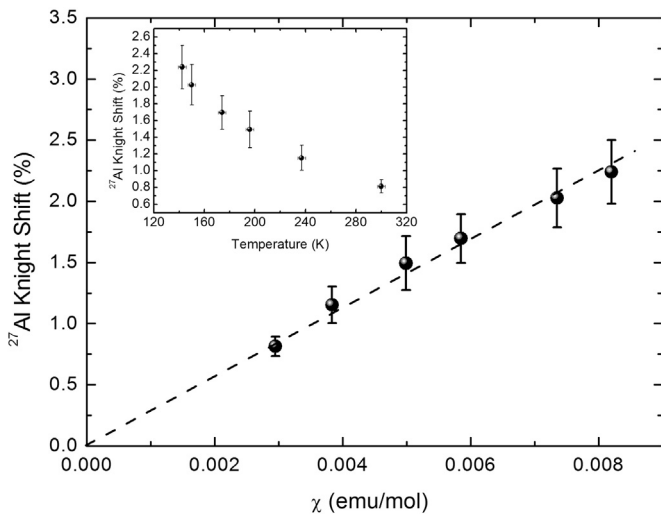


Fig. 6. Evolution of the  $^{27}\text{Al}$  Knight shift ( $^{27}\text{K}$ ) as a function of temperature (inset) and bulk susceptibility  $\chi_{\text{bulk}}$ .

$$^{27}\text{K}(T) \approx K_0 + \frac{A_{\text{HF}}}{N_A \mu_B} \chi(T)$$

where  $K_0$  is the Knight shift at  $\chi=0$ ,  $A_{\text{HF}}$  is the hyperfine coupling constant,  $N_A$  is the Avogadro number,  $\mu_B$  the Bohr magneton and  $\chi$  the bulk magnetic susceptibility. Using this definition, the  $A_{\text{HF}}$  value obtained is equal to  $1.567 \text{ kOe}/\mu_B$  and the  $K$ - $\chi$  slope to  $281 \text{ (mol emu}^{-1}\text{)}$ . Moreover, at  $K_0 \sim 0$ , therefore, there is no contribution of the spin operator to the Van Vleck term at the Al sites. Even though the previously defined hyperfine coupling constant is the real physical property used to define the effect of the hybridization with the f-electrons, several definitions are used and we therefore preferred to consider directly the value of the  $K$ - $\chi$  slope ( $\alpha$ ). Arko et al. found  $\alpha$  values of 2.9 and  $11.2 \text{ (mol emu}^{-1}\text{)}$  for  $\text{UAl}_2$  and  $\text{PuAl}_2$  respectively which are very small compared to that found in  $\text{NpAl}_2$ . By contrast, a value in the same range of order was found for the metallic ferromagnetic  $\text{UGa}_2$  ( $290 \text{ mol emu}^{-1}$ ) [35].

The other NMR parameter which strongly varies when

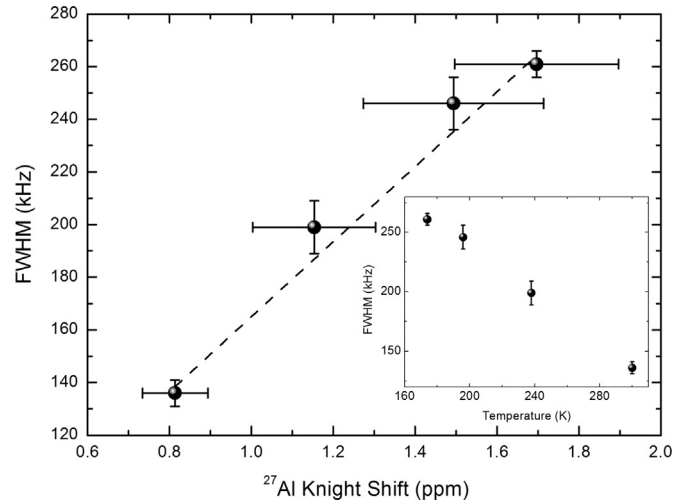


Fig. 7. Evolution of the line broadening (FWHM) against the  $^{27}\text{Al}$  Knight shift.

decreasing the temperature is the line broadening, FWHM, has observed in inset of Fig. 7. For a better understanding of the origin of the FWHM broadening with temperature, a plot with K has been made. In fact, if a linear correlation is obtained, the variation of NMR line width is caused by a distribution of internal static fields at the Al sites due to the  $\text{Np}^{3+}$  magnetic moments [36,37]. The linear relation between FWHM and K clearly demonstrates that the observed line broadening here mainly arises from the magnetic dipolar interaction. Therefore, this important linear increase of the central transition linewidth with temperature seems to confirm the sensing of the ferromagnetic correlation already at room temperature as mentioned above.

Finally, for the range of temperatures under study, a constant spin-lattice relaxation time ( $T_1$ ) of about 1 ms was found. Additional experiments using NQR instead of NMR should be very relevant especially for the confirmation of the ferromagnetic fluctuations with  $T_1$  or the study in the ferromagnetic state.

#### 4. Conclusion

In this paper, we report the results of a renewed investigation of the magnetic properties of the ferromagnetic  $\text{NpAl}_2$  compound using magnetic susceptibility and  $^{27}\text{Al}$  NMR spectroscopy. The magnetic transition is very well established at  $T_C = 56 \text{ K}$ . An effective moment of  $\mu_{\text{eff}} = 2.1 \mu_B/\text{Np}$  was obtained by magnetic susceptibility in agreement with previous work. The full  $^{27}\text{Al}$  NMR spectrum of  $\text{NpAl}_2$  (i.e. central and satellite transitions) at room temperature was determined for the first time. By lowering the temperature, the  $^{27}\text{Al}$  NMR spectra show strong temperature dependence of the Knight shift in the paramagnetic state suggesting the presence of ferromagnetic fluctuations on the  $^{27}\text{Al}$  nuclei above  $T_C$ . No variations of  $\nu_Q$  were observed with temperatures excluding the possibility of lattice distortion. Besides, comparison of the  $K$ - $\chi$  plot suggests higher s-f hybridization for  $\text{NpAl}_2$  than  $\text{UAl}_2$  and  $\text{PuAl}_2$ . The influence of the ferromagnetic fluctuations on this parameter can nevertheless not be excluded. The origin of the line broadening which strongly varied with temperature was attributed to static distribution of K based on the linear variation of the FWHM-K plot.

This low temperature NMR analysis of such highly radioactive material is the first of a kind in JRC-ITU and therefore opens several routes for magnetic studies of these unique and very intriguing 5f-bearing compounds.

**Acknowledgments**

We are thankful to Thomas Poumeyrol for fruitful discussions about the VOCS technique. The high purity Np metal required for the fabrication of the compound was made available through a loan agreement between Lawrence Livermore National Laboratory and ITU, in the framework of a collaboration involving LLNL, Los Alamos National Laboratory and the US Department of Energy.

**References**

- [1] P. Santini, S. Carretta, G. Amoretti, R. Caciuffo, N. Magnani, G.H. Lander, *Rev. Mod. Phys.* **81** (2009) 807.
- [2] K. Moore, G. van der Laan, *Rev. Mod. Phys.* **81** (2009) 235.
- [3] K. Ikushima, S. Tsutsui, Y. Haga, H. Yasuoka, R.E. Walstedt, N.M. Masaki, A. Nakamura, S. Nasu, Y. Onuki, *Phys. Rev. B* **63** (2001) 104404.
- [4] K. Ikushima, H. Yasuoka, S. Tsutsui, S. Nasu, N.M. Masaki, A. Nakamura, Y. Ueda, *Physica B* **281–282** (2000) 197–199.
- [5] H. Yasuoka, G. Koutroulakis, H. Chudo, S. Richmond, D.K. Veirs, A.I. Smith, E. D. Bauer, J.D. Thompson, G.D. Jarvinen, D.L. Clark, *Science* **336** (2012) 901–904.
- [6] N.J. Curro, T. Caldwell, E.D. Bauer, L.A. Morales, M.J. Graf, Y. Bang, A.V. Balatsky, J.D. Thompson, J.L. Sarrao, *Nature* **434** (2005) 622–625.
- [7] S. Kambe, Y. Homma, Y. Tokunaga, H. Sakai, D. Aoki, E. Yamamoto, A. Nakamura, Y. Shiokawa, R.E. Walstedt, *Physica B* **359–361** (2005) 1072–1074.
- [8] S. Kambe, H. Sakai, Y. Tokunaga, R.E. Walstedt, D. Aoki, Y. Homma, Y. Shiokawa, *Phys. Rev. B* **76** (2007) 144433.
- [9] Y. Tokunaga, D. Aoki, Y. Homma, H. Sakai, H. Chudo, S. Kambe, T.D. Matsuda, S. Ikeda, E. Yamamoto, A. Nakamura, Y. Haga, Y. Shiokawa, Y. Onuki, *J. Phys. Soc. Jpn.* **77** (Suppl. A) (2008) S211–S213.
- [10] Y. Tokunaga, S. Kambe, H. Sakai, H. Chudo, T.D. Matsuda, Y. Haga, H. Yasuoka, D. Aoki, Y. Homma, Y. Shiokawa, Y. Onuki, *Phys. Rev. B* **79** (2009) 054420.
- [11] A.T. Aldred, B.D. Dunlap, D.J. Lam, I. Nowik, *Phys. Rev. B* **10** (1974) 1011.
- [12] A.T. Aldred, B.D. Dunlap, G.H. Lander, *Phys. Rev. B* **14** (1976) 1276–1282.
- [13] A.J. Arko, F.Y. Fradin, M.B. Brodsky, *Phys. Rev. B* **8** (1973) 4104–4118.
- [14] F. Wilhelm, R. Eloirdi, J. Ruzs, R. Springell, E. Colineau, J.–C. Griveau, P. M. Oppeneer, R. Caciuffo, A. Rogalev, G.H. Lander, *Phys. Rev. B* **88** (2013) 024424.
- [15] A.M. Boring, R.C. Albers, G.R. Stewart, D.D. Koelling, *Phys. Rev. B* **31** (1985) 3251–3259.
- [16] E. Colineau, J.P. Sanchez, F. Wastin, P. Javorsky, E. Riffaud, Y. Homma, P. Boulet, J. Rebizant, *J. Phys.: Condens. Matter* **20** (2008) 255234.
- [17] E. Colineau, P. Gaczynski, J.–C. Griveau, R. Eloirdi, R. Caciuffo, *Hyperfine Interact.* **207** (2012) 113–120.
- [18] F.Y. Fradin, Nuclear Magnetic Resonance and the question of 5f electron localization in the actinides, In: *Proceedings of 2nd International Conference on the Electronic Structure of the Actinides*, Wroclaw, Poland, 13–16 1976, September.
- [19] D. Aoki, Y. Haga, T.D. Matsuda, N. Tateiwa, S. Ikeda, Y. Homma, H. Sakai, Y. Shiokawa, E. Yamamoto, A. Nakamura, R. Settai, Y. Onuki, *J. Phys. Soc. Jpn.* **77** (Suppl. A) (2008) S159–S164.
- [20] H. Chudo, H. Sakai, Y. Tokunaga, S. Kambe, D. Aoki, Y. Homma, Y. Shiokawa, Y. Haga, S. Ikeda, T.D. Matsuda, Y. Onuki, H. Yasuoka, *J. Phys. Soc. Jpn.* **77** (2008) 083702.
- [21] K. Gofryk, J.–C. Griveau, E. Colineau, J.P. Sanchez, J. Rebizant, R. Caciuffo, *Phys. Rev. B* **79** (2009) 134525.
- [22] D. Massiot, I. Farnan, N. Gautier, D. Trumeau, A. Trokner, J.P. Coutures, *Solid-State Nucl. Magn. Reson.* **4** (1995) 241–248.
- [23] D. Massiot, F. Fayon, M. Capron, I. King, S. Le Calvé, B. Alonso, J.O. Durand, B. Bujoli, Z. Gan, G. Hoatson, *Magn. Reson. Chem.* **40** (2002) 70–76.
- [24] A.T. Aldred, *J. Magn. Magn. Mater.* **10** (1979) 53.
- [25] L. Manes, L. Manes, C.K. Jorgensen, U. Benedict, M.S.S. Brooks, J.M. Fournier, J. Ghijsen, W. Müller, J.R. Naegele, J.–C. Spirlet, *Actinides – Chemistry and Physical Properties (Structure and Bonding 59/60)*, Springer, 1985, p. 164.
- [26] K.J.D. Mackenzie, M.E. Smith, *Multinuclear Solid-state NMR of Inorganic Materials*. Pergamon Material Series.
- [27] A.C. Gossard, V. Jaccarino, J.H. Wernick, *Phys. Rev.* **128** (1962) 1038.
- [28] F.Y. Fradin, M.B. Brodsky, A.J. Arko, *J. Phys. Colloque C1 Tome 32 (supplément au no. 2–3)* (1971) C1-905.
- [29] D.E. MacLaughlin, O. Pena, M. Lysak, *Phys. Rev. B* **23** (1981) 1039.
- [30] K. Kang, M. Lee, *Curr. Appl. Phys.* **14** (2014) 383–388.
- [31] E.D. Jones, J.I. Budnick, *J. Appl. Phys.* **37** (1966) 1250–1251.
- [32] N.M. Wolcott, R.L. Falge, L.H. Bennett, R.E. Watson, *Phys. Rev. Lett.* **21** (1968) 546–549.
- [33] A. Prasad, V.K. Anand, U.B. Paramanik, Z. Hossain, R. Sarkar, N. Oeschler, M. Baenitz, C. Geibel, *Phys. Rev. B* **86** (2012) 014414.
- [34] B. Chen, H. Ohta, C. Michioka, Y. Itoh, K. Yoshimura, *Phys. Rev. B* **81** (2010) 134416.
- [35] S. Kambe, H. Sakai, Y. Tokunaga, Y. Haga, E. Yamamoto, *J. Phys. Soc. Jpn.* **83** (2014) 114710.
- [36] R.E. Walstedt, L.R. Walker, *Phys. Rev. B* **9** (1974) 4857.
- [37] C.N. Kuo, C.S. Lue, Z. Heb, M. Itoh, *Solid State Commun.* **149** (2009) 341–344.